Two-dimensional crystals of streptavidin on biotinylated lipid layers and their interactions with biotinylated macromolecules

Seth A. Darst,* Michael Ahlers,‡ Paul H. Meller,‡ Elizabeth W. Kubalek,* Rainer Blankenburg,‡ Hans O. Ribi,* Helmut Ringsdorf,‡ Roger D. Kornberg*

*Beckman Laboratories, Fairchild Center, Department of Cell Biology, Stanford University School of Medicine, Stanford, California 94305 USA; and ‡Institut für Organische Chemie, Universität Mainz, D-6500 Mainz, FRG

ABSTRACT Streptavidin forms two-dimensional crystals when specifically bound to layers of biotinylated lipids at the air/water interface. The three-dimensional structure of streptavidin determined from the crystals by electron crystallography corresponds well with the structure determined by x-ray crystallography. Comparison of the electron and x-ray crystallographic structures reveals the occurrence of free biotin-binding sites on the surface of the two-dimensional crystals facing the aqueous solution. The free biotin-binding sites could be specifically labeled with biotinylated ferritin. The streptavidin/biotinylated lipid system may provide a general approach for the formation of two-dimensional crystals of biotinylated macromolecules.

INTRODUCTION

Both optical and electron microscopy have been used to investigate structures of, and interactions between, proteins and lipids at the air/water interface (1–3). These methods are most revealing when protein molecules at the interface are organized in crystalline arrays. Such two-dimensional crystals are readily formed at the air/water interface (3, 4). Crystallization depends upon specific protein binding to natural or synthetic lipid-ligands incorporated into planar lipid films. Bound proteins are concentrated and oriented in two-dimensions by virtue of specific binding and are free to move into regular lattice positions due to lateral diffusion of lipids in a fluid film. Two-dimensional crystals have been obtained by this approach with a monoclonal anti-dinitrophenyl antibody bound to a lipid-linked dinitrophenyl moiety (4), with the B1 subunit of *Escherichia coli* ribonucleotide reductase bound to lipid-linked dATP (5), and with cholera toxin bound to its natural membrane receptor, ganglioside GM_1 (6).

Despite the variety of systems to which the lipid-layer crystallization approach has been applied, the requirement for a specific lipid-ligand in each case is a limitation. The formation of two-dimensional crystals of *E. coli* RNA polymerase holoenzyme on positively charged lipid layers (7) demonstrates one way of circumventing this difficulty. Positively charged lipid layers, lacking any specific ligands, bind RNA polymerase through electrostatic interactions in a manner conducive to crystallization. While modification of the lipid properties such as electrostatic charge may prove fruitful in other instances, success in the case of RNA polymerase was probably dependent on special properties of the protein, so this strategy may not be widely applicable. There remains the need for a general adaptor molecule that utilizes specific binding to link a wide variety of macromolecules to lipid layers without the requirement for a specific lipid-ligand in each case.

Here we address the need for a general adaptor through studies of streptavidin from *Streptomyces avidinii*, a tetrameric protein with four sites of very high affinity binding to biotin (8). It has been shown by fluorescence microscopy that the interaction of streptavidin with biotinylated lipids in monolayers leads to the formation of large protein domains with diameters up to 200 μm (9). Here we report the formation and electron microscopic analysis of two-dimensional crystals of streptavidin on lipid layers containing biotinylated lipid. Structural and direct binding studies reveal free biotin-combining sites on the surface of the lipid-bound streptavidin. These results suggest that streptavidin can serve as a general adaptor molecule for biotinylated lipid layers through interactions of these sites with a broad range of biotinylated molecules.

MATERIALS AND METHODS

Materials

The five biotinylated lipids used in this study (Fig. 1, *top*), *N*-biotinyl(*S*-[1,2-bis[octadecyloxycarbonyl]ethyl]cysteine (1), *N*-biotinyl-*S*-1-carboxy-2-([*N*,*N*- dioctadecylamino)carbonyl)ethyl)cysteine (2), *N*-biotinyl-*S*-1-phosphatidyl-3-glycero-*sn*-dimyristyl (3), *N*,*N*-dioctadecyl-*N'*-biotinyl-propanediamine (4), and *N*,*N*-dioctadecyl-biotinamide (5) were synthesized as described (9). Streptavidin was from Sigma Chemical Co. (St. Louis, MO) or from Dianova (Hamburg, FRG). Ferritin (type I from horse spleen), biotinylated ferritin (type I from horse spleen, 7 mol biotin/mol ferritin), biotin, and fluorescein isothiocyanate (FITC)[1]

[1]*Abbreviations used in this paper:* FITC, fluorescein isothiocyanate; NBD-PC, 1-palmitoyl-2-[*N*-(7-nitro-2,1,3-benzo-oxadiol-4-yl)aminocaproyl] phosphatidylcholine; SOPC, 1-stearoyl-2-oleoyl phosphatidylcholine.

0006-3495/91/02/387/10 $2.00

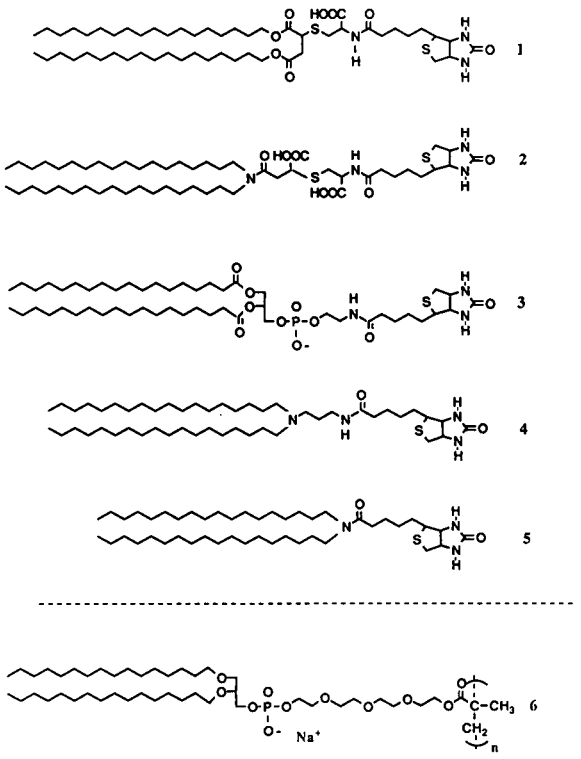

FIGURE 1 (*Top*) Structures of the five biotinylated lipids used in this study. (*Bottom*) Structure of the polymeric amphiphile used to coat the electron microscope grids.

were from Sigma Chemical Co. 1-stearoyl-2-oleoyl phosphatidylcholine (SOPC)[1] and 1-palmitoyl-2-[*N*-(7-nitro-2,1,3-benzo-oxadiol-4-yl)aminocaproyl] phosphatidylcholine (NBD-PC)[1] were from Avanti Polar Lipids (Birmingham, AL). The labeling of streptavidin with FITC was performed as described by Nargessi and Smith (10). The procedure results in a labeling density of about one fluorescein molecule per streptavidin molecule. The polymeric amphiphile sodium-bis(hexadecyloxy)propyl-1,2-methacryloyl-3,6,9,12 tetraoxadecyl phosphate (6; Fig. 1, *bottom*) was synthesized according to Elbert et al. (11).

Two-dimensional crystallization

Ordered arrays were prepared either on droplets coated with lipid or in a miniaturized Langmuir monolayer trough (12) as follows.

Droplet method

At 30°C, droplets (10 μl) of streptavidin solution (100–250 μg/ml in 50 mM Tris, pH 7.0, 150 mM NaCl) were placed in Teflon wells (4 mm diam., 0.5 mm deep) and the surfaces of the droplets coated with 0.5–1 μl of a lipid mixture containing 0.1 mg biotinylated lipid/ml and 0.4 mg SOPC/ml in chloroform/hexane (1:1, vol/vol). The droplets were incubated at 30°C in a humid chamber for ~30 min. Carbon-coated electron microscope grids were then placed on top of the wells with the carbon surface contacting the droplet, withdrawn, washed with one drop of distilled water, and stained for 15–30 s with 1% (wt/vol) uranyl acetate.

Langmuir trough technique

A chloroform solution of lipid with a total lipid concentration of 0.1 mg/ml was spread at room temperature at the air/water interface of the Langmuir trough containing a subphase buffer of 50 mM Tris, pH 7.0, 150 mM NaCl. After evaporation of the solvent and equilibration, monolayers were compressed to either the fluid-expanded phase (1–6 mN/m, compounds 1–4) or to the condensed phase of the biotinylated lipid (30–40 mN/m, compounds 1–3). Streptavidin, or FITC-streptavidin, dissolved in buffer solution, was injected through the lipid layer into the subphase to a final concentration of 10–100 μg/ml. To follow the growth of protein/lipid domains, the preparations were performed in the Langmuir trough on the stage of an epi-fluorescence microscope (13). The visualization of the domains could be achieved by doping the lipid monolayer with small amounts of a fluorescent lipid probe (< 1 mol% NBD-PC) or by the use of FITC-streptavidin. In both cases, the growth of large fluorescent domains (50–100 μm in length) was observed. With FITC-streptavidin, the domains exhibited a pronounced polarization anisotropy (Fig. 2). An incubation time of 10 min to 3 h at room temperature (pure biotinylated lipids) or at 30°C (mixtures with SOPC) was used for the formation of the two-dimensional domains. With the use of FITC-streptavidin, the fluorescent domains could be observed after only a few minutes. Removal of the grids and negative staining were performed as described above.

Different methods were used to transfer the lipid/protein domains onto electron microscope grids: (*a*) Carbon-coated grids were placed onto the surface of the lipid monolayer and removed horizontally. (*b*) Hydrophilic grids (carbon-coated and glow discharged for 1 min in vacuum) were either withdrawn vertically from beneath the aqueous subphase, or the grids were placed horizontally on a support underneath the subphase and the layer at the air/water interface was deposited on the grid by slowly removing the liquid subphase. This method leaves the protein layer in direct contact with the grid surface (rather than the lipid layer). (*c*) A single monolayer of a polymeric amphiphile (compound 6) was transferred onto carbon-coated, glow discharged grid surfaces by Langmuir Blodgett deposition (14), with the hydrophilic portion of the amphiphilic layer in contact with the grid surface, in an attempt to produce a more stable, homogeneous, and well-defined hydrophobic surface. This homopolymer has been extensively investigated and was shown earlier to produce ordered and homogeneous layers on solid supports (11, 15, 16). The transfer process was performed with control of the surface pressure at 30 ± 1 mN/m. In a second step, the polymer-coated electron microscope grids were passed vertically through the protein/lipid layer on the surface of a trough, the air/water interface was cleared of protein and lipid, and the grids were withdrawn from the subphase horizontally through the interface (Fig. 3). The grids were then negatively stained with uranyl acetate as described above.

For labeling with biotinylated ferritin (or ferritin as control), streptavidin crystals were prepared and transferred to an electron microscope grid by method *a* above, washed with one drop of distilled water, then incubated with a drop of ferritin solution (100 μg/ml in 10 mM Tris, pH 7.4, 150 mM NaCl) for 2–5 min. The grids were then washed with another drop of distilled water and stained with 1% uranyl acetate.

Electron microscopy and image processing

For structure determination, only data obtained from crystals on biotinylated lipid 1 were used. Electron micrographs were recorded at a calibrated magnification of 27,800× with a Philips EM400 at 100 kV on Kodak SO163 film. Three micrographs from each crystalline area were recorded using low electron doses (< 10 e/Å^2), two with the specimen tilted with respect to the incident 100-kV electron beam, and

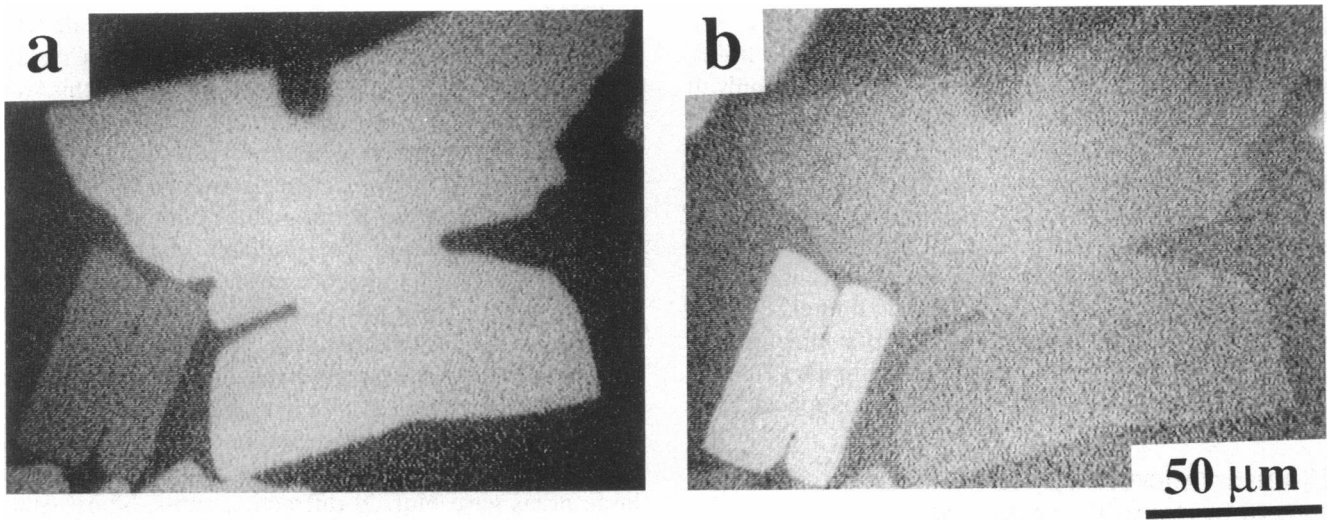

FIGURE 2 Fluorescent domains formed by FITC streptavidin attached to a monolayer of lipid 5 at 30°C. Each image was recorded using a linear polarizer. The position of the linear polarizer in *a* is 90° with respect to its position in *b*.

one untilted. Micrographs of test areas showed that no noticeable degradation in the diffraction data occurred after three exposures, even for the highest resolution spots observed.

Micrographs of similar quality were selected by optical diffractometry and digitized on a Perkins-Elmer autodensitometer with a 20-μm square aperture and step size, corresponding to 7.2 Å on the image. The data were then processed by computer using standard methods (17). Additional computations were performed incorporating procedures for correcting lattice distortions by reciprocal space filtering, real space correlation analysis, and spline function interpolation as described by Henderson et al. (18). The position of the tilt axis and tilt angle were obtained by the method of Shaw and Hills (19). The Fourier terms obtained were combined according to the crystallographic space group P2 and smooth curves were fit to the amplitude and phase data (20). The Fourier terms for calculation of a three-dimensional map were collected by sampling these curves at intervals of 0.00667 $Å^{-1}$ in z^*.

RESULTS

Fluorescence microscopy reveals ordered domains of streptavidin on biotin-lipid monolayers

All five of the biotinylated lipids tested supported the formation of two-dimensional domains of FITC-streptavidin as determined by fluorescence microscopy. Depending on the biotinylated lipid used and the experimental conditions, different domain morphologies could be generated. These ranged from smooth, rectangular, or "H"-like shapes to dendritic patterns (9). Under identical conditions of subphase composition, temperature, and protein concentration, the formation of fluorescent domains with different biotinylated lipids showed a strong dependence on the lipid structure and the surface

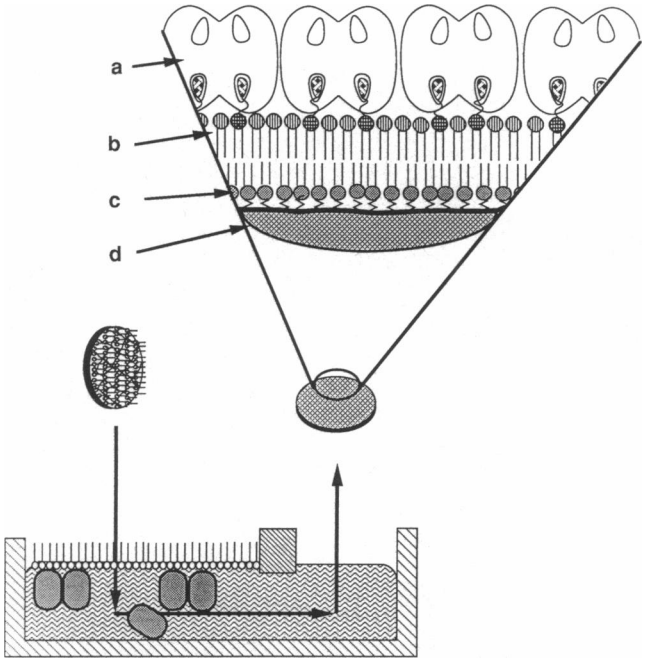

FIGURE 3 Schematic illustration of grid preparation method 3 (see text). The grid, coated with carbon and then with a monolayer of an amphiphilic polymer, is lowered vertically through a monolayer of biotinylated lipids with bound streptavidin at the air/water interface of a Langmuir trough. The grid, along with deposited biotinylated lipids and streptavidin, is then withdrawn through the uncoated air/water interface. (*a*) bound streptavidin molecules, (*b*) monolayer containing biotinylated lipids, (*c*) monolayer of amphiphilic polymer adsorbed to grid surface, and (*d*) carbon-coated grid surface.

pressure. Whereas domain formation was possible with compounds 1 and 2 in the condensed phase of the lipids, domain formation using compound 4 took place only in the fluid-expanded phase. Using lipid 5, domains could only be formed in the initial isothermal region of the gas-analogue/fluid-expanded phase transition. In all cases where the emitted fluorescence of the domains was generated by FITC streptavidin, a pronounced optical anisotropy was observed by observation through linear polarizors (Fig. 2). The formation of fluorescent domains did not occur when FITC streptavidin was exposed to monolayers of nonbiotinylated lipids (9), indicating that the protein-lipid interaction was specific.

Electron microscopy reveals two-dimensional crystals of streptavidin on biotin-lipid layers

Two-dimensional crystals of streptavidin were formed either in droplets coated with lipid layers containing biotinylated lipid or in the aqueous subphase of a Langmuir trough with a lipid monolayer containing biotinylated lipid. With the use of method *a* described above for crystal transfer to carbon-coated grids, crystalline areas up to $\sim 10\ \mu m^2$ in area were revealed by electron microscopy (Fig. 4 and Fig. 5 *a*). Crystals transferred to the electron microscope grid in this way often appeared to be derived from much larger domains at the air/water interface that were broken apart by stresses involved in the transfer process (Fig. 4). This idea is consistent with the far greater dimensions (up to 100 μm in length) of the domains observed at the air/water interface by fluorescence microscopy. With polymer-coated grids and using the Langmuir-Blodgett transfer method (method *c* above), crystalline areas up to 30 μm in length were observed. Unfortunately, such large areas transferred onto polymer-coated grids did not exhibit good long-range order, as determined by optical diffraction from the electron micrographs. These large areas gave blurred diffraction spots. Sharp spots could be obtained by choosing smaller areas for diffraction. Method *b* gave similar results to method *c*. In general, crystals produced in the Langmuir trough were larger but less abundant on the electron microscope grids than those produced in droplets. There was no apparent difference in the degree of order of the negatively stained crystals produced by the different methods. Edge views, obtained when lipid layers, along

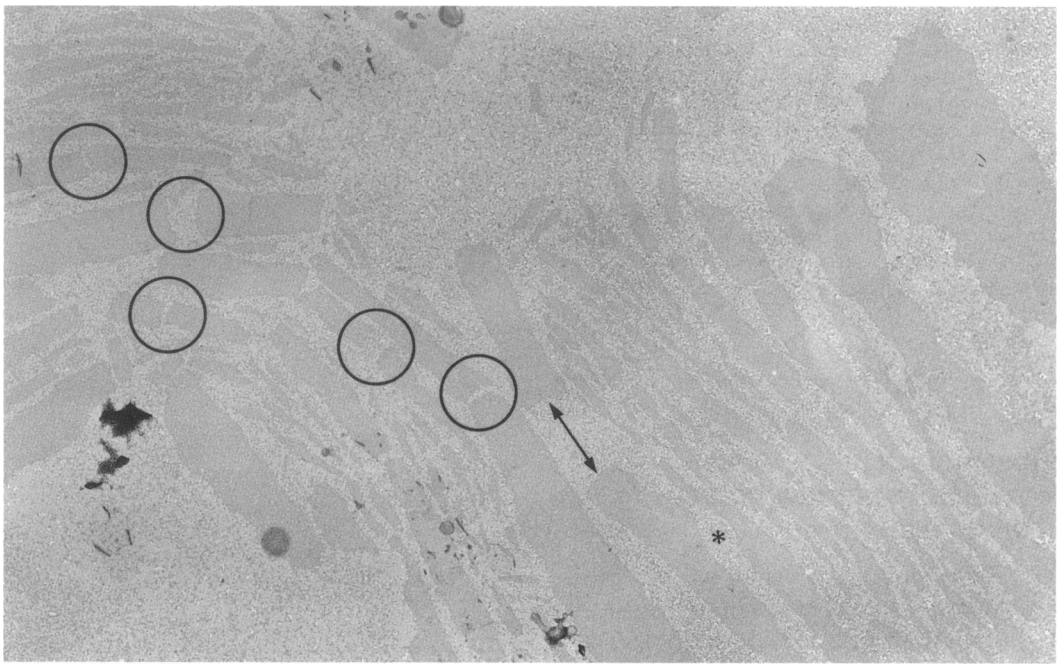

FIGURE 4 Electron micrograph of streptavidin on biotinylated lipid 1/SOPC layers transferred to a carbon-coated electron microscope grid and stained with 1% uranyl acetate. The bottom edge of the micrograph corresponds to 20 μm. Highly ordered, two-dimensional arrays of streptavidin are seen as dark patches against a lighter, mottled background. At this low magnification, the ordered lattice is not discernible (see Fig. 5 *a*). The ordered domains appear to have been parts of a much larger domain that was broken apart, probably by stresses involved in the transfer from the air/water interface to the carbon surface of the grid. This is illustrated by examples of cracks that appear to have formed between domains that were once joined (*circles*), or domains that appear to have been broken apart and drifted away from each other (*arrow*), or long, adjacent surfaces of domains that appear to fit against each other like the pieces of a jigsaw puzzle (*).

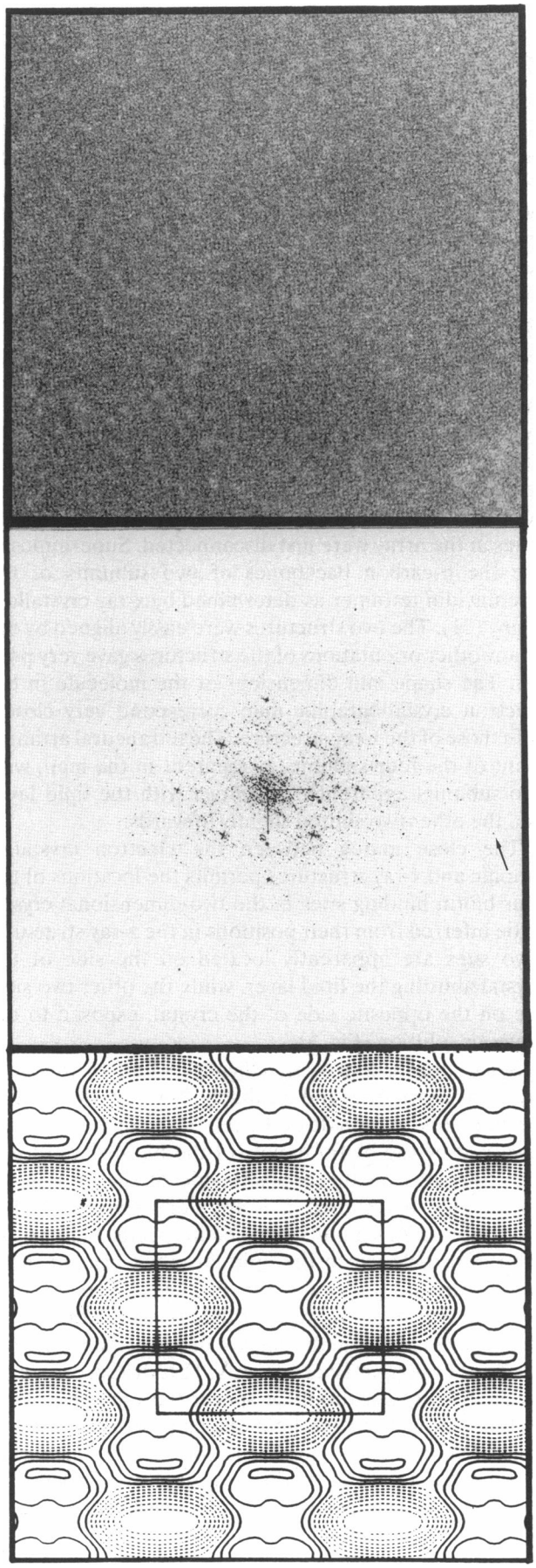

with bound protein crystals, fortuitously folded away from the grid, showed that the crystals consisted of a single layer of streptavidin molecules with a thickness of ~50 Å (images not shown).

The crystals diffracted in negative stain (Fig. 5 *b*) and had average unit cell parameters $a = 84 \pm 1$ Å, $b = 85 \pm 2$ Å, and $\gamma = 90 \pm 1°$. The (1, 5) reflection (at 16.7 Å resolution) is clearly visible by eye in the diffraction pattern (Fig. 5 *b*). The square lattice, the systematic absences for $(h + k)$ odd, the apparent *mm* symmetry of the diffraction pattern, and the known tetrahedral symmetry of streptavidin (21) all suggested that the crystals belonged to the crystallographic space group C222. Two-dimensional projection maps were calculated from an average of eight noise-filtered Fourier transforms corrected for lattice distortions. Refining all reflections with amplitudes greater than twice background with the assumption of P2 symmetry resulted in an average phase error of 5.3° to a resolution of 14.2 Å. Assuming C222 symmetry a phase error of 7.7° and an amplitude R factor of 0.3 was obtained. A map assuming C222 symmetry (Fig. 5 *c*) revealed streptavidin molecules ~55 × 45 Å.

As with other proteins crystallized by the lipid-layer method (3), two-dimensional crystals of streptavidin formed under a wide range of conditions such as protein concentration (10–250 μg/ml) and temperature (20–50°C). With the five different biotinylated lipids, the results obtained by electron microscopy correlated well with those from fluorescence microscopy. The five biotinylated lipids vary in the charge of the head group and in the hydrophilic spacer length between the functional biotin moiety and the hydrophobic alkyl chains. Biotin lipids 1–3 contain long hydrophilic spacers, while lipid 4 has only a short spacer. In the case of lipid 5, where the biotin moiety is directly linked to the hydrophobic alkyl chains, there is no spacer element. Biotinylated lipids 1–4 supported the formation of ordered, fluorescent domains of FITC streptavidin that could be transferred to electron microscope grids and identified by electron microscopy as two-dimensional crystals. With lipid 5,

FIGURE 5 (*top*) Electron micrograph of an ordered array of streptavidin on biotinylated lipid 1/SOPC layers stained with 1% uranyl acetate. The bottom edge of the micrograph corresponds to 0.73 μm. (*middle*) Computed diffraction pattern, after correction for lattice distortions, of the crystalline area in *a*. The reciprocal lattice vectors **a*** and **b*** are indicated. The (1, 5) refection, at 16.7 Å resolution, is clearly visible (*arrow*). Diffraction to 14.2 Å is present in the digitized and averaged data from several images. (*bottom*) Two-dimensional projection map calculated from the noise-filtered Fourier transforms corrected for lattice distortions and with the assumption of C222 symmetry. The unit cell is indicated. The map represents the averaged data from eight images containing a total of ~10,000 molecules. The bottom of the map corresponds to 200 Å.

however, domains were observed by fluorescence microscopy but no crystalline areas were found after transfer to electron microscope grids, either because the domains were not truly crystalline or because they did not survive the transfer process.

When streptavidin was incubated in the absence of lipid, no crystals could be found either on hydrophobic or hydrophilic (glow discharged) carbon-coated grids. When biotinylated lipid was omitted, some protein binding but no crystallization was observed on the SOPC layers, demonstrating that concentration and orientation of the protein by specific binding to lipid-linked biotin is a prerequisite for crystallization. This requirement was further demonstrated by experiments with streptavidin saturated with biotin. When streptavidin was treated for ~15 min at 30°C with a slight excess (20 nM) of biotin, followed by incubation with biotinylated lipid/SOPC layers, protein binding to the lipid layers occurred but no highly ordered, square lattices were observed. Poorly ordered hexagonal arrays of protein were occasionally seen which were probably due to hexagonal close packing of nonspecifically adsorbed molecules. This phenomenon has been observed with other protein/lipid systems and illustrates that care must be taken in the case of hexagonal arrays before they are identified as true crystals, even when such arrays appear to be highly ordered (6).

Square lattices, once formed on biotinylated lipid/SOPC layers, could be exposed to up to ~20 nM biotin in solution for a few minutes without effect. Exposure to a concentration of 200 nM biotin for 1 min, however, disrupted the crystals. Streptavidin may have a significantly higher affinity for biotin in solution than for the biotinylated lipid in planar layers.

Three-dimensional structure of streptavidin/biotinylated lipid complex reveals free biotin binding sites

A total of 34 micrographs of crystals tilted at angles from 0° to 49° with respect to the incident electron beam were used to reconstruct the three-dimensional structure of the streptavidin/biotinylated lipid 1 complex. The images were processed and combined according to the crystallographic space group P2 using standard methods (17). Although, as indicated above and as suggested by the resulting P2 map, the crystals show C222 space group symmetry, we computed the structure in space group P2 to avoid averaging differences in staining between the top, exposed surface of the crystals and the bottom lipid-associated surface. The average phase error, based on refinement of each new measurement with all previously accumulated, symmetry-related phases within 0.005 $Å^{-1}$ in z^*, was 12°. No single micrograph had an average phase error > 19°. A least squares procedure (20) was used to fit smooth curves to the combined amplitude and phase data for each of the 26 independently determined lattice lines included in the reconstruction (Fig. 6). 124 Fourier terms were used to calculate the three-dimensional map. Terms out to 12 Å resolution in the $x^* - y^*$ plane were included in the reconstruction. Due to the limited data in the z^* direction, the resolution perpendicular to the plane of the crystal is estimated to be ~20 Å.

A single streptavidin tetramer from the calculated map is viewed obliquely from above in Fig. 7, with the lipid layer lying beneath. The contour level shown defines the negative stain-excluding region and thus reflects the surface topography of the molecule. This contour level was chosen such that the individual molecules in the array were just disconnected. Superimposed are the α-carbon backbones of two subunits of the streptavidin tetramer as determined by x-ray crystallography (21). The two structures were easily aligned by eye as any other orientations of the structures gave very poor fits. The shape and dimensions of the molecule in the electron crystallographic map correspond very closely with those of the x-ray structure. The tetrahedral arrangement of the four subunits is apparent in the map, with two subunits apparently in contact with the lipid layer and the other two shifted slightly upwards.

The close match between the electron crystallographic and x-ray structures permits the locations of the four biotin binding sites in the two-dimensional crystal to be inferred from their positions in the x-ray structure. Two sites are apparently located on the side of the crystal abutting the lipid layer, while the other two sites are on the opposite side of the crystal, exposed to the aqueous solution (Fig. 8).

Since streptavidin is specifically bound to the lipid layer, at least one and probably both of the biotin-binding sites on the side of the crystal facing the lipid are occupied by the biotin moiety of the biotinylated lipid. The two sites on the opposite side of the crystal are presumably unoccupied. It is apparent from Fig. 8 that the streptavidin subunits involved in specific binding are not the two closest to the lipid layer but instead those shifted slightly up away from the layer. The distance between the carbonyl group of the bound biotin moiety, which pokes out from the surface of the protein, and the surface of the lipid layer is ~8 Å. This distance must be spanned by the hydrophilic spacer between the biotin carbonyl group and the lipid chains of the biotinylated lipid. This notion is consistent with our findings that biotinylated lipids 1–3, with long hydrophilic spacers, supported crystallization well under a broad range of surface pressures (up to 40 mN/m), while biotinylated

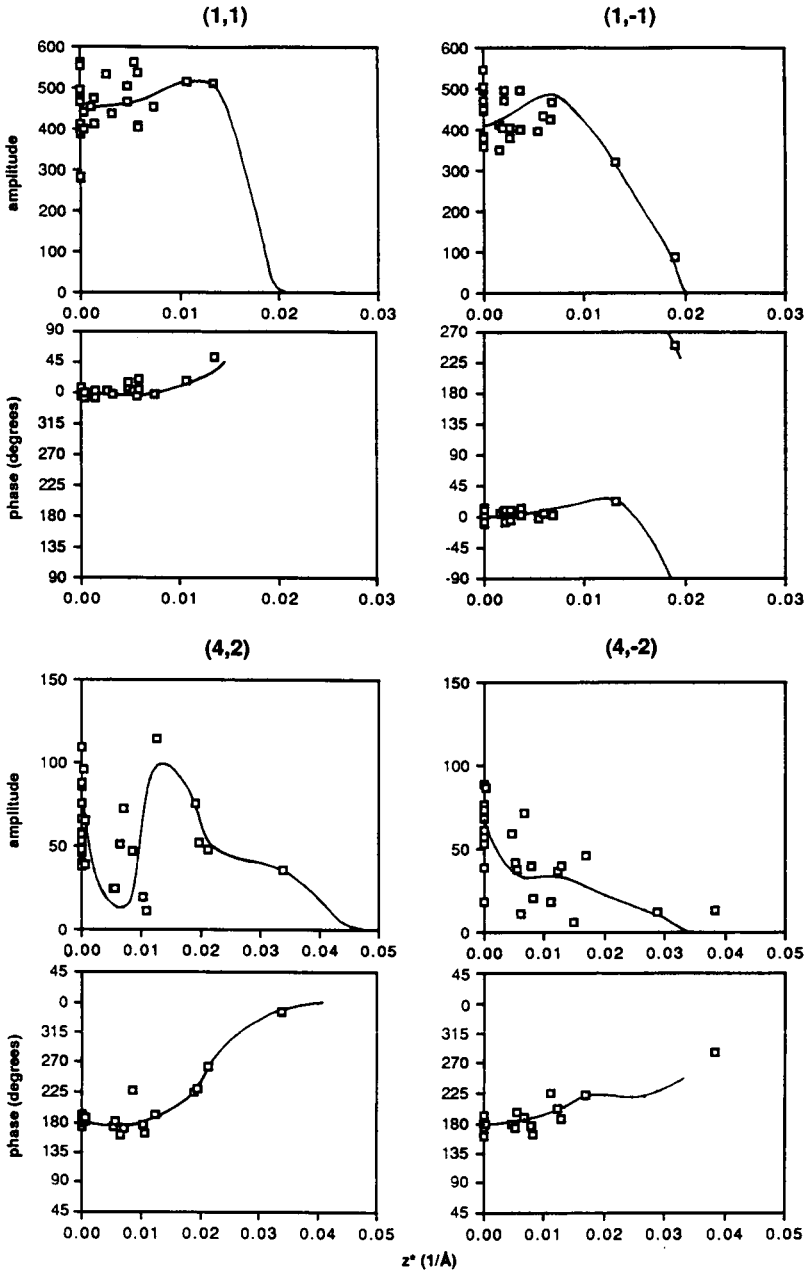

FIGURE 6 Values of amplitude and phase determined along selected reciprocal lattice lines from micrographs of specimens tilted to the incident beam by angles up to 49°. z^* is the distance in reciprocal space in the direction of the c^* axis, perpendicular to the plane of the lattice. The data have been combined in space group P2. The smooth curves (*solid lines*) through the data were determined by a least squares procedure (20).

lipid 4, with a short spacer, supported crystallization only in the fluid-expanded phase, where the protein could more easily insert between the lipid molecules. Finally, lipid 5, with no spacer, supported the formation of fluorescent protein domains only in a noncompressed monolayer. It is unclear whether these domains were crystalline because no ordered areas were recovered after transfer to electron microscope grids.

Free biotin-binding sites on streptavidin crystals can interact with biotinylated ferritin

The inferrence from structural studies that biotin-binding sites are exposed on the surface of the streptavidin crystals and are available for interaction with biotinylated macromolecules was tested as follows. Streptavidin

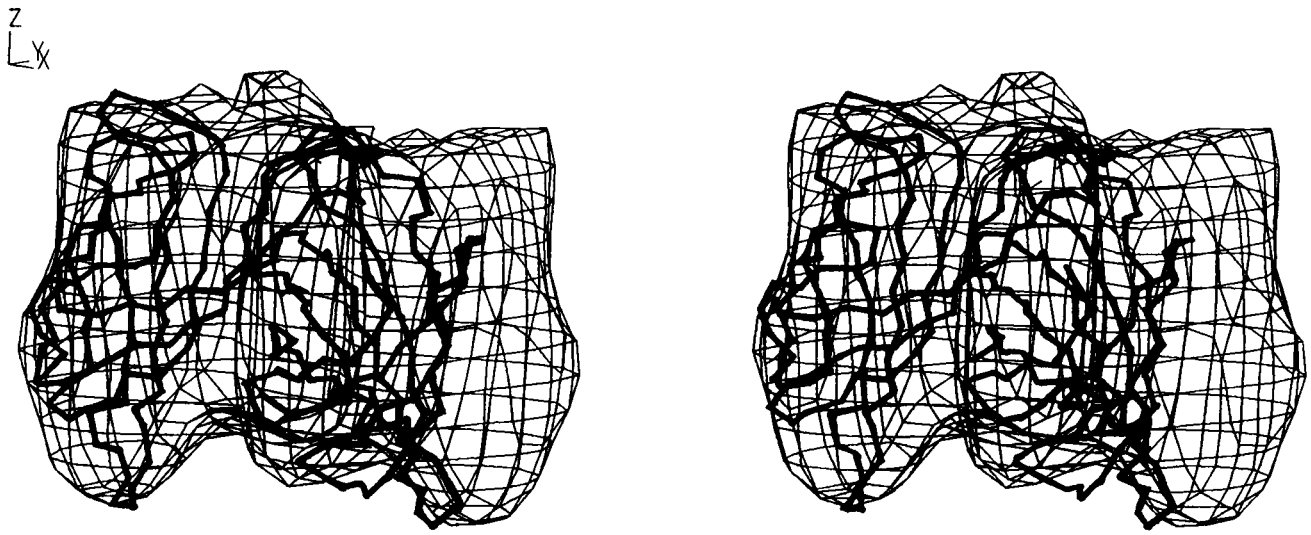

FIGURE 7 Stereo view of a computer generated model of a single streptavidin tetramer viewed at an oblique angle from above the lipid layer. The α-carbon backbones of two subunits of the streptavidin tetramer, determined by x-ray crystallography (21), are superimposed (*thick lines*) to illustrate the close match between the structures determined by the different methods. The other two subunits of the x-ray structure are omitted for clarity. The crystallographic *a* and *b* axes correspond to the *x* and *y* axes, respectively, which are indicated. The *z* axis is perpendicular to the plane of the lipid layer. The models of Figs. 6 and 7 were generated using the program FRODO (22) on an Evans and Sutherland color graphics system.

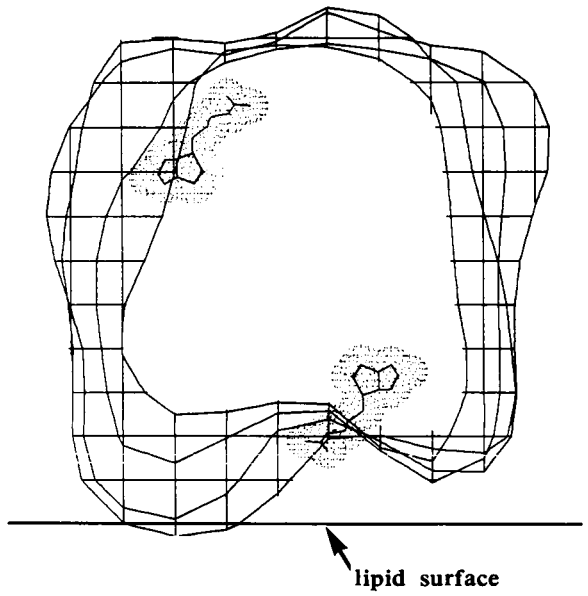

FIGURE 8 An approximately 12-Å thick slice of the electron density map viewed directly along the crystallographic *a* axis. The slice, which contains two biotin-binding sites, is shown with biotin molecules superimposed in the positions (inferred from the x-ray structure) they would occupy if the sites were filled. The approximate position of the lipid layer is indicated. The other two biotin-binding sites are related by a two-fold rotation in the plane of the lipid layer. The horizontal lines delineating the structure are separated by 4 Å.

crystals were formed, transferred to an electron microscope grid, and incubated with 100 μg/ml biotinylated ferritin. Negative staining and electron microscopy revealed streptavidin crystals heavily labeled with ferritin molecules (Fig. 9). Areas of lipid containing bound but unordered streptavidin were also labeled with the biotinylated ferritin. Increasing the concentration of biotinylated ferritin in the incubation step resulted in streptavidin crystals labeled with higher densities of ferritin, but it then became difficult to recognize the streptavidin lattice underneath the ferritin molecules. In identical experiments with ferritin instead of biotinylated ferritin, virtually no binding to either streptavidin crystals or to bound but unordered streptavidin was observed, indicating that labeling with biotinylated ferritin was specific. When streptavidin bound to biotinylated lipid was incubated first with 20 nM biotin to saturate the free biotin-binding sites and then with biotinylated ferritin, no labeling was observed, further indicating that the binding of biotinylated ferritin was specific.

DISCUSSION

We have demonstrated that large, well-ordered, two-dimensional crystals of streptavidin can be formed by specific binding to lipid layers containing biotinylated lipid. The formation of ordered domains of fluorescein-

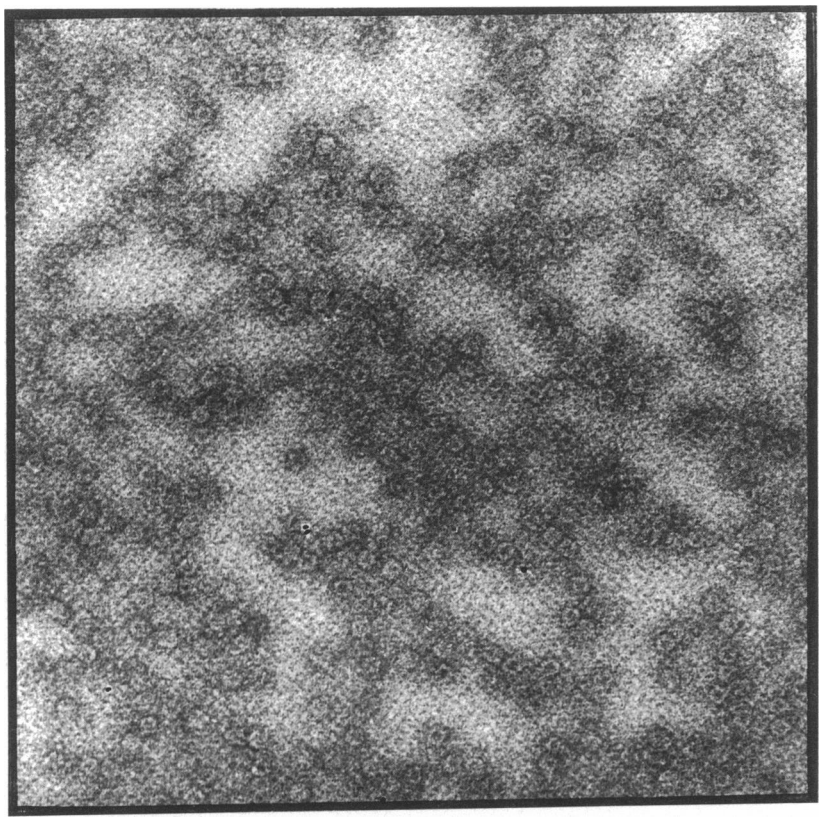

FIGURE 9 Electron micrograph of a negatively stained, ordered array of streptavidin labeled with biotinylated ferritin (100 μg/ml) by incubation for 2 min. The bottom edge of the micrograph corresponds to 0.53 μm.

ated streptavidin on monolayers containing biotinylated lipid has been demonstrated by fluorescence microscopy and polarization anisotropy (9). The crystals transferred onto carbon-coated grids and observed by electron microscopy were much smaller than the ordered domains seen on the lipid monolayers at the air/water interface by fluorescence microscopy (4 μm^2 as compared with 2,500 μm^2). Crystal transfer onto amphiphilic polymer-coated grids by Langmuir-Blodgett deposition resulted in the transfer of crystalline areas up to 30 μm in length and a dramatically increased fraction of the grid surface area was covered with crystalline areas.

The accessibility of the lipid-linked biotin moieties to the binding site of streptavidin is influenced by the length of the hydrophilic spacer between the hydrophobic alkyl chains of the lipid and the biotin moiety and also by the surface pressure of the lipid monolayer. Whereas lipids 1–3, with long hydrophilic spacers, bind streptavidin while in a densely packed phase (30–40 mN/m), FITC-streptavidin domain formation with lipid 4, having a short hydrophilic spacer, can only be achieved in the fluid-expanded phase. Monolayers consisting of lipid 5, with the functional biotin moiety directly linked to the alkyl chains, exhibit fluorescent domains only in noncompressed monolayers at close to 0 mN/m. At high surface pressures when the monolayer is in a condensed state, a long spacer is required for streptavidin to reach the biotin moieties. In the expanded phase, the protein can insert partly into the lipid monolayer, allowing binding to biotin moieties with shorter spacers. This explanation is consistent with earlier observations of an increase in the surface pressure of monolayers of biotinylated lipid after injection of streptavidin in the subphase (9).

The match between the surface of streptavidin revealed by electron crystallography and the envelope of the x-ray structure is remarkably close. Thus, at least in this case there are no gross artefacts caused by negative staining or by the missing cone of Fourier space not sampled due to the upper limit on tilt angle in the electron microscope. The quality of the electron crystallographic structure is more than adequate to allow the

inference that two biotin-binding sites of the streptavidin tetramer face away from the lipid layer, exposed to the aqueous solution.

The specific binding of biotinylated ferritin to the exposed sites on a streptavidin crystal points to the possible use of streptavidin as a general adaptor for linking biotinylated macromolecules to lipid layers. While the biotinylated ferritin bound to the streptavidin crystals did not form ordered arrays, this was not expected for two reasons. First, the biotinylated ferritin contained on average 7 mol biotin/mol ferritin and so was not uniquely oriented by binding to streptavidin. Second, the biotinylated ferritin was bound to preformed streptavidin crystals and thus lateral diffusion could not occur.

We thank Wayne A. Hendrickson, Arno Pähler and colleagues for providing us with their crystal structure of streptavidin before its publication.

The costs of this research were paid by National Institutes of Health grants AI21144 and GM30387 to Dr. Kornberg. Dr. Darst was supported by an American Cancer Society Postdoctoral Fellowship.

Received for publication 11 May 1990 and in final form 13 August 1990.

REFERENCES

1. McConnell, H. M., L. Tamm, and R. M. Weiss. 1984. Periodic structures in lipid monolayer phase transitions. *Proc. Natl. Acad. Sci. USA.* 81:3249–3253.
2. Jarvis, L. R. 1988. Microcomputer video image analysis. *J. Microsc.* 150:83–97.
3. Kornberg, R. D., and H. O. Ribi. 1987. Formation of two-dimensional crystals of proteins on lipid layers. *In* Protein Structure, Folding, and Design 2. D. L. Oxender, editor. Alan R. Liss, Inc., New York. 175–186.
4. Uzgiris, E. E., and R. D. Kornberg. 1983. Two-dimensional crystallization technique for imaging macromolecules, with an application to antigen-antibody-complement complexes. *Nature (Lond.).* 301:125–129.
5. Ribi, H. O., P. Reichard, and R. D. Kornberg. 1987. Two-dimensional crystals of enzyme-effector complexes: ribonucleotide reductase at 18 Å resolution. *Biochemistry.* 26:7974–7979.
6. Ludwig, S. D., H. O. Ribi, G. K. Schoolnik, and R. D. Kornberg. 1986. Two-dimensional crystals of cholera toxin B subunit-receptor complexes: projected structure at 17 Å resolution. *Proc. Natl. Acad. Sci. USA.* 83:8585–8588.
7. Darst, S. A., H. O. Ribi, D. W. Pierce, and R. D. Kornberg. 1988. Two-dimensional crystals of *Escherichia coli* RNA polymerase holoenzyme on positively charged lipid layers. *J. Mol. Biol.* 203:269–273.
8. Green, N. M. 1975. Avidin. *Adv. Protein Chem.* 29:85–133.
9. Blankenburg, R., P. Meller, H. Ringsdorf, and C. Salesse. 1989. Interaction between biotin lipids and streptadivin in monolayers: formation of oriented two-dimensional protein domains induced by surface recognition. *Biochemistry.* 28:8214–8221.
10. Nargessi, R. D., and D. S. Smith. 1986. Fluorometric assays for avidin and biotin. *Methods Enzymol.* 122:67–72.
11. Elbert, R., A. Laschewsky, and H. Ringsdorf. 1985. Hydrophilic spacer groups in polymerizable lipids: formation of biomembrane models from bulk polymerized lipids. *J. Am. Chem. Soc.* 197:4134–4141.
12. Meller, P. 1989. Microspectroscopy on single domains of phase-separated monolayers. *J. Microsc.* 156:241–246.
13. Meller, P. 1988. Computer-assisted video microscopy for the investigation of monolayers on liquid and solid substances. *Rev. Sci. Instrum.* 59:2225–2231.
14. Gaines, G. L. Jr. 1966. Insoluble monolayers at liquid-gas interphases. John Wiley & Sons, Inc., New York. 1–383.
15. Laschewsky, A., H. Ringsdorf, G. Schmidt, and J. Schneider. 1987. Self-organization of polymeric lipids with hydrophilic spacers in side groups and main chain: investigation of monolayers. *J. Am. Chem. Soc.* 109:788–796.
16. Meller, P., R. Peters, and H. Ringsdorf. 1989. Microstructure and lateral diffusion in monolayers of polymerizable amphiphiles. *Colloid Polym. Sci.* 267:97–107.
17. Amos, L. A., R. Henderson, and P. N. T. Unwin. 1982. Three-dimensional structure determination by electron microscopy of two-dimensional crystals. *Prog. Biophys. Mol. Biol.* 39:183–231.
18. Henderson, R., J. M. Baldwin, K. H. Downing, J. Lepault, and F. Zemlin. 1986. Structure of purple membrane from *Halobacterium halobium:* recording, measurement and evaluation of electron micrographs at 3.5 Å resolution. *Ultramicroscopy.* 19:147–178.
19. Shaw, P. J., and G. J. Hills. 1981. Tilted specimen in the electron microscope: a simple specimen holder and the calculation of tilt angles for crystalline specimens. *Micron.* 12:279–282.
20. Agard, D. A. 1983. A least-squares method for determining structure factors in three-dimensional tilted-view reconstructions. *J. Mol. Biol.* 167:849–852.
21. Hendrickson, W. A., A. Pähler, J. L. Smith, Y. Satow, E. A. Merritt, and R. P. Phizackerley. 1989. Crystal structure of core streptavidin determined from multiwavelength anomalous diffraction of synchrotron radiation. *Proc. Natl. Acad. Sci. USA.* 86:2190–2194.
22. Jones, T. A. 1978. A graphics model building and refinement system for macromolecules. *J. Appl. Cryst.* 11:268–272.